DOI: https://doi.org/10.68732/2e5352a463b302f8

ISBN: 978-9989-2053-7-8

Feature extraction and classification of spatially varying rock mass around a circular tunnel using CNN

P. Mishra
Research Scholar, Indian Institute of Technology Kharagpur, Kharagpur, West Bengal, India
pratishtham22@kgpian.iitkgp.ac.in
0009-0002-7996-4066

D. Chakraborty
Associate Professor, Indian Institute of Technology Kharagpur, Kharagpur, West Bengal, India
0000-0002-9383-9539

Abstract

This study aims to quantify the rotational anisotropic behavior of spatially variable rock slope mass in the presence of a tunnel. The rock mass is assumed to follow the Generalized Hoek-Brown (GHB) failure criterion, adhering to rock strength metrics such as the Geological Strength Index (*GSI*), the uniaxial compressive strength of intact rock (σ_{ci}), and the intact rock constant (m_i). The random fields of uniaxial compressive strength (σ_{ci}) of rock mass are prepared using lower-bound random finite element limit analysis (LB-RFELA). The random fields generated are assumed to follow a log-normal distribution, and the rock properties are horizontally stratified. These fields are prepared using the Markovian autocorrelation function and the expansion optimal linear estimation (EOLE). Initially, a full-fledged numerical approach is performed to develop the random fields using random field theory (RFT) and Monte Carlo Simulation (MCS). The surcharge (q_s) over the rock slope domain is optimized, and a dataset of input random field realizations, along with their corresponding stability numbers, is prepared. A convolutional neural network (CNN) is developed that extracts complex features, including erratic stratifications and their interactions with varying slope angles. Henceforth, the model predicts the stability of the rock slope domain embedded with a tunnel. The results show that the model reliably identifies the tunnel, slope angles, and autocorrelation lengths. Because the study emphasizes probabilistic behavior, key stratification parameters, particularly autocorrelation lengths, were incorporated during CNN development. The model's predictions were compared with those from the rigorous numerical procedure, and the close agreement confirms the CNN's efficiency in capturing spatial variability and anisotropic effects.

Keywords

Random field theory, EOLE, Tunnel, Hoek-Brown slope, CNN.

1 Introduction

Slopes are dominant, naturally occurring geostructures, and analyzing their stability is of prime importance, as evidenced by the specific subject of slope stability analysisincluded in geotechnical engineering textbooks (Lambe& Whitman, 2008; Craig, 2013). Additionally, tunnel construction in mountainous regions has increased due to high transportation and utilitarian demands. Tunnels are complex structures, and when embedded in a slope, they trigger intricate mechanisms that alter the original distribution of stresses in the slope. Many studies have conducted stability analyses of tunnels embedded in horizontal or sloping soil (Sloan & Assadi, 1991; Yamamoto et al., 2011; Chakraborty & Kumar, 2013). Additionally, geomaterials are prone to uncertainties due to years of deposition, loading history, and mineral composition. These uncertainties, if unattended, affect the structure's strength and design, which are either under or over-estimated. A reliability analysis was conducted to assess the stability of the geotechnical structures and address this setback. This analysis is conducted in two ways: the simpler approach treats the strength and deformation parameters of the relevant problem as random variables to calculate the structure's collapse load for all realizations. In contrast, the more sophisticated method treats these parameters as a random field and varies them spatially across all considered realizations. The latter methodology subsequently captures the fundamental nature of field occurrences and stochastically accounts for the maximum potential scenarios that may lead to structural failure. Many studies have accounted for the spatially varying nature of the geomaterial, thereby reducing the risk associated with the geostructure of interest, such as a tunnel embedded in spatially varying soil (Ali et al., 2017; Pan et al., 2019). Later, tunnel stability was assessed in ahomogeneous Hoek-Brown rock mass (Rahaman & Kumar, 2020). A few studies examine tunnels in spatially varying rock masses to incorporate the intrinsic uncertainties of the rock mass. (Pan et al. 2019; Chen et al. 2019). Apart from rigorous physics-based computations, few AI/ML models have emerged to study the behavior of geotechnical problems and predict stability by developing relations between input features and outputs, such as response surface methods, artificial neural networks, emotional neural networks, functional neural networks, decision trees, etc. These models require a continuous or discontinuous array of features to understand the subject's behavior and predict the stability ratio or safety factor (problem-specific) (Babu & Srivastava, 2008; Bharti et al., 2021; Mishra et al, 2021). Later, researchers developed an enhanced technique using computer vision to extract features from the image rather than an array of numbers. This ensured that, based on the literature and experimental data, if a field condition is simulated, the images prepared from the probabilistic numerical analysis can be fed into the prepared model, which can then map the important features and predict the system's stability. This model is called a convolutional neural network (CNN). A few studies have been conducted to analyze the stability of the system (strip footing resting on aspatially varying soil domain, spatially varying slope, tunnel surrounded by spatially varying rock mass, etc.) based on random field images prepared from the probabilistic analysis (Fu et al., 2022; Mishra & Chakraborty, 2024; Zhang et al., 2021).

The abovementioned studies explain the importance of assessing the tunnel and slope; however, when these two structures are treated as one system, the mechanics at play become complex, as now the tunnel failure is not symmetric, the overburden is more at the mountain side, which creates a bias of pressure changing the failure mechanism. Therefore, this study examines the behavior of a tunnel embedded in a spatially varying slope. Thereafter, it aims to prepare a CNN model that extracts features from random fields, study the interactions among the slope, the tunnel, and the horizontal anisotropy, and classify whether the system is stable or unstable.

2 Deterministic analysis

A plane strain mesh domain is created using three-noded triangular elements, which is shown in Fig. 1. The deterministic analysis of a tunnel at a depth $H/D = 2$ is performed for ground inclinations of β = 0°, 10°, and 20° relative to the horizontal. The domain's width and height were chosen to ensure no yielding at the boundaries, regardless of the increase in the strength parameters. The Hoek-Brown parameters considered in this study are GSI = 20, 40, 60, and 80; m_i = 5, 10, 15, and 20; and the disturbance factor DF = 0.5, as the rock mass is considered to be medium disturbed. The dimensionless ratio $\sigma_{ci}/\gamma D$ = 1000, and the unit weight is taken as 25 kN/m^3. The surcharge ($q_s/\gamma D$) over the whole domain is optimized by employing a lower-bound finite element limit analysis (LB-FELA) (Sloan, 1988). Astatically admissible stress field is generated, which satisfies the specified equilibrium and boundary conditions (Fig. 1). Also, it is ensured that stress continuity is maintained across the shared edges of adjacent elements and that it does not violate the yield criterion, which is

the Hoek-Brown criterion in this problem. The optimization technique incorporated into the study to compute the collapse surcharge load is power cone programming (PCP) (Kumar & Rahaman, 2020), which is explained in equations 1-13. The GHB yield criterion is expressed as follows:

$$\sigma_1 - \sigma_3 - (m_b \sigma_1 (\sigma_{ci})^{(1-\alpha)/\alpha} - s(\sigma_{ci})^{1/\alpha})^{\alpha} \leq 0 \tag{1}$$

where σ_1 and σ_3 are the major and minor principal stresses, m_b, s, and α are functions of *GSI*, m_i, and *DF* as stated by (Kumar & Rahaman, 2020).

The yield criterion given in eq. 1 is further dissociated and assembled in the form of conic constraints of second-order conic programming (SOCP) and PCP, which is as follows:

$$\text{SOCP: } x_3^2 + x_2^2 \leq x_1^2 \tag{2}$$

$$\text{PCP: } x_4^{\alpha} x_5^{1-\alpha} \geq \sqrt{x_6^2} \tag{3}$$

Where x_1, x_2, x_3, x_4, x_5, and x_6 are the conic constants.

Thereafter, q_s is maximized when subjected to

$$\left[A_{equalities}\right]\{\lambda\} = \{b_{equalities}\} \tag{5}$$

$$\left[A_{inequalities}\right]\{\lambda\} = \{b_{inequalities}\} \tag{6}$$

Equation 5 is built by combining the equilibrium condition, boundary condition, and discontinuity condition, whereas equation 6 consists of the yield criterion. Vector $\{\lambda\} = \{\sigma, q_s, x\}$ where σ is the array of global nodal stresses, q_s is the surcharge pressure to be optimized, and x is the array of conic constants.

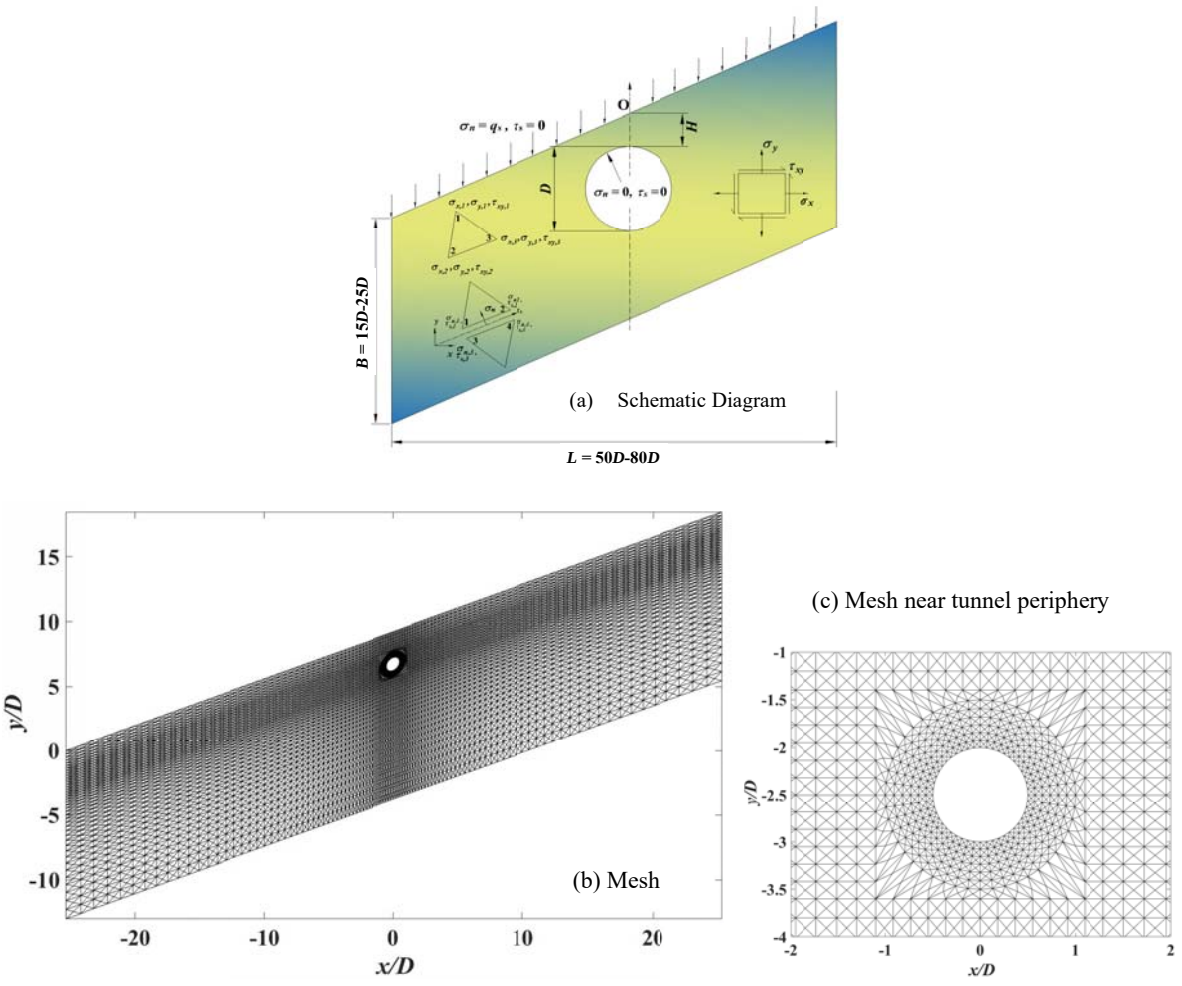


Fig. 1 Schematic diagram and mesh view of the domain.

3 Random field discretization

The first step towards incorporating probabilistic analysis is to discretize the random field, i.e., assign a strength value to each domain element. Sudret and Kiureghian (2000) explained that discretization methods fall into three categories: point discretization, spatial averaging, and series expansion (Der Kiureghian& Ke, 1988; Spanos & Ghanem, 1989; Vanmarcke& Grigoriu, 1983). Series expansion methods approximate the random field using deterministic and probabilistic functions. The methodology adopted in this study is expansion optimal linear estimation (EOLE) (Li & Der Kiureghian, 1993), which is based on optimal linear estimation (OLE) or kriging, which aims to estimate the soil property at an unsampled location from sampled experimental data using linear estimation. However, in EOLE, the correlation matrix undergoes spectral decomposition, and the entire field is discretized based on the dominant eigenvalues. This methodology modeled random fields that are Gaussian and uncorrelated. Later, Vořechovský (2008) extended this methodology to the general case of cross-correlated non-Gaussian random field cases.The methodology adopted in this paper first prepares an autocorrelation matrix using the Markovian first-order exponential anisotropic autocorrelation functionρ^{NG}.

$$\rho^{NG} = \exp\left(-\frac{dx}{l_x} - \frac{dy}{l_y} \right) \tag{7}$$

where l_x and l_y are the autocorrelation lengths in horizontal and vertical direction, and *dx* and *dy* are the centroidal distances between two elements.Equation 7 is used to prepare the non-Gaussian autocorrelation matrix ∑NG, which is then transformed into the Gaussian matrix $\sum^G$ using the Nataf transformation. Furthermore, the discretization takes place as follows:

$$\widetilde{Z} = \mu_{\ln Z} + \sigma_{\ln Z} \sum_{i=1}^{N} \frac{\kappa_i}{\sqrt{\lambda_i}} . \phi_i \Delta \tag{8}$$

$\widetilde{Z}$ is the random field for N retained values. μ_{lnZ} and σ_{lnZ} are the mean and standard deviation of the underlying Gaussian random field. After the spectral decomposition of $\sum^G$, λ_i, and ϕ_i are the eigenvalues and eigenvectors retained. κ_i is the vector of standard normal variables, and Δ is the correlation vector between an arbitrary coordinate. It is to be noted that *N* is determined by sorting the eigenvalues in descending order and selecting the prominent eigenmodes that contribute to higher interaction, based on a 10% tolerance for variance error. A detailed explanation of the methodology can be found in Al-Bittar and Soubra (2017). The parameters adopted for the probabilistic analysis are given in Table 1. The random fields prepared for different autocorrelation lengths and slopes are given in Fig. 2.

Table 1. Parameter values adopted in this study.

Parameters	**Values**
D	1 m
H/*D*	2
GSI	40
m_i	15
σ_{ci}	25 MPa
$\sigma_{ci}/\gamma D$	1000
l_x/D	10
l_y/D	0.5, 5, 10
$COV_{\sigma ci}$	0.25

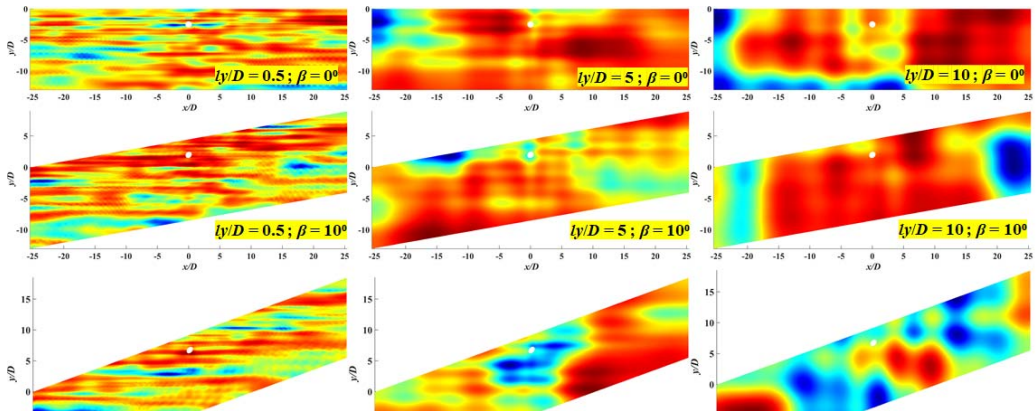


Fig. 2 Random field contours.

4 Feature extraction and stability prediction (CNN)

The probabilistic and deterministic analyses, in themselves, are tedious procedures that require precision to capture the inherent uncertainties of geomaterials. Many AI/ML algorithms have been introduced to reduce the effort required to develop a clear relation between soil uncertainties and stability, which sometimes lie beyond the engineering scope and require assumptions. Numerous researchers have introduced neural networks or other ML modelsthat simulate the problem with a human intelligence prerogative (Goh et al., 2018; Zhang et al., 2019; Saikia et al., 2020). With advances in the technical field of recognizing inherent uncertainties and their patterns, and studying their effects on the geostructure, deep learning has also developed models that examine the correlation between spatially varying parameters by treating them as vectors and relating them to the stability number. This led to a loss of the pattern in the profile of the geomaterial. To address this setback, several studies examined the features of the pixel in an artificial image, a simulation of the real field scenario (Wang & Goh, 2021; Zhang et al., 2021). This study, however, aims to examine the interaction between the tunnel and the slope, as well as spatial variability, and to classify a particular simulation of the problem as stable or unstable. The prepared model is given in Figure 3. It describes the deep neural network used to study the features of the complex images shown in Figure 2.

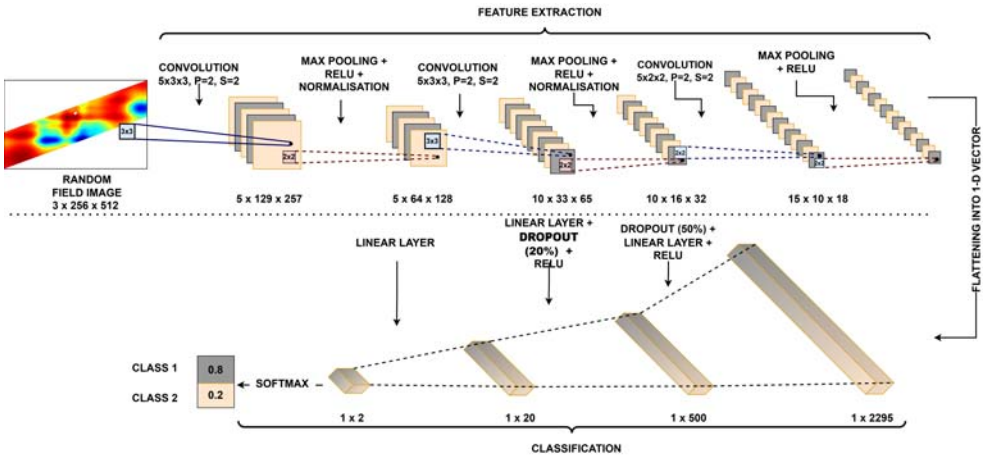


Fig. 3 Architecture of CNN.

5 Results and conclusion

This study primarily examines the stability ofa tunnel embedded in an infinite rock slope. It was observed that, for an increase in tunnel embedment depth, the stability number increases as the cover depth over the tunnel crown increases, allowing a larger area to mobilize strength. An increase in the strength parameters, i.e., *GSI* and m_i, leads to a more stable tunnel-slope system, providing greater strength for mobilization and failure. Also, it was observed that with an increase in the slope inclination, the stability decreases, which is quite intuitive, as there is non-uniformity in the cover depth over the crown on both sides. This asymmetrical arrangement shifts the maximum depth away from the crown and to another position of the tunnel's periphery, reducing the strength of the slope-

tunnel system. After the core deterministic analysis, probabilistic analysis was performed, and it was observed that the mean probabilistic stability number followed the same trend as the deterministic value. Also, with an increase in the autocorrelation length, the probability of failure decreased, as at lower autocorrelation, the failure tends to occur from a weak plane recurring at a shorter distance, increasing the number of cases prone to failure. Later, CNN was prepared with three layers of convolution, max pooling, and ReLU, and the extracted features were then used for classification.

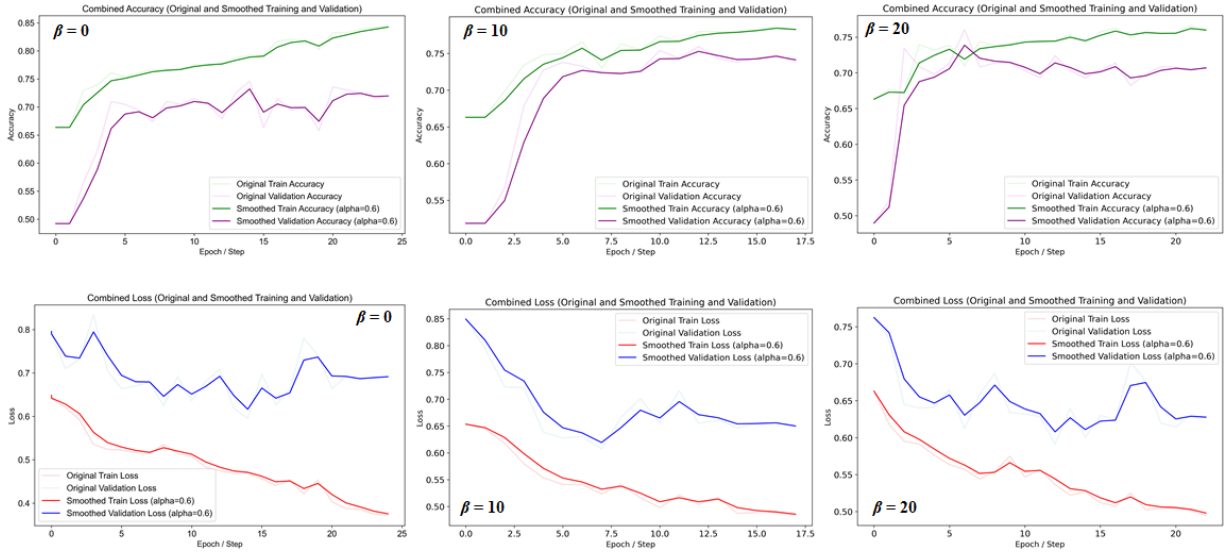


Fig. 4 Accuracy and Loss vs Epoch plots.

Figure 4 shows the accuracy and loss vs epoch plots for the model trained for different slope angles. Enlisted are the conclusions from the results:

- The plots show that the model was trained for only a few epochs, compared to 100 when it was run; it stopped learning after a few epochs, producing a straight line with no learning gradient.
- It was observed that the training accuracy may increase after a few epochs, while the validation loss was either unaffected or even increasing, leading to overfitting.
- The training accuracy decreases with increasing slope angle; for β = 0°, the model's accuracy was 82.24% on the training set and 71.77% on the validation set. Similarly, for β = 10° and 20°, the model's accuracy was 78.16% and 75.84% for training, and 68.11% and 68% for validation.
- With an increase in the slope angle, the stratification behavior changes, affecting tunnel stability. The model has scope to improve accuracy by adding more data to the dataset while preserving the data's variability.
- Geomaterials are inherently uncertain, and with proper geological surveys and experimental tests, ground data is made available; this deep learning model can then be further expanded to real field data with available profiles for testing.
- This study is a baseline examination to reduce the rigorous technical efforts included in the physics-based formulation of the stability of different geostructures.

This study aims to analyze the stability of an infinite rock slope embedded with a tunnel by developing a CNN model for a preliminary geological site survey using available site-specific data. Also, it has future scope to analyze different discontinuities within the rock mass and provide a full-fledged model that studies the rock profile for faults, folds, bedding planes, etc.

References

Al-Bittar, T., & Soubra, A. H. (2017). Bearing capacity of spatially random rock masses obeying Hoek–Brown failure criterion. *Georisk: Assessment and Management of Risk for Engineered Systems and Geohazards*, *11*(2), 215-229.

Ali, A., Lyamin, A. V., Huang, J., Sloan, S. W., & Cassidy, M. J. (2017). Undrained stability of a single circular tunnel in spatially variable soil subjected to surcharge loading. *Computers and Geotechnics*, *84*, 16-27.

Babu, G. S., & Srivastava, A. (2008). Response surface methodology (RSM) in the reliability analysis of geotechnical systems. *Proc., 12th International Association for Computer Methods and Advances in Geomechanics*, 4147-4165.

Bharti, J. P., Mishra, P., Moorthy, U., Sathishkumar, V. E., Cho, Y., & Samui, P. (2021). Slope stability analysis using Rf, gbm, cart, bt and xgboost. *Geotechnical and Geological Engineering*, *39*(5), 3741-3752.

Chakraborty, D., & Kumar, J. (2013). Stability of a long unsupported circular tunnel in soils with seismic forces. *Natural Hazards*, *68*(2), 419-431.

Chen, F., Wang, L., & Zhang, W. (2019). Reliability assessment on stability of tunnelling perpendicularly beneath an existing tunnel considering spatial variabilities of rock mass properties. *Tunnelling and Underground Space Technology*, *88*, 276-289.

Craig, R. F. (2013). *Soil mechanics*. Springer.

Der Kiureghian, A., & Ke, J. B. (1988). The stochastic finite element method in structural reliability. *Probabilistic engineering mechanics*, *3*(2), 83-91.

Fu, Y., Lin, M., Zhang, Y., Chen, G., & Liu, Y. (2022). Slope stability analysis based on big data and convolutional neural network. *Frontiers of Structural and Civil Engineering*, *16*(7), 882-895.

Goh, A. T. C., Zhang, W., Zhang, Y., Xiao, Y., & Xiang, Y. (2018). Determination of earth pressure balance tunnel-related maximum surface settlement: a multivariate adaptive regression splines approach. *Bulletin of Engineering Geology and the Environment*, *77*(2), 489-500.

Lambe, T. W., & Whitman, R. V. (2008). *Soil mechanics SI version*. John Wiley & Sons.

Mishra, P., & Chakraborty, D. (2024, September). Meta-model Based Probabilistic Study of a Strip Footing Placed over a Spatially Varying Rock Mass. In *Asian Rock Mechanics Symposium* (pp. 285-294). Singapore: Springer Nature Singapore.

Mishra, P., Samui, P., & Mahmoudi, E. (2021). Probabilistic design of retaining wall using machine learning methods. *Applied Sciences*, *11*(12), 5411.

Pan, Y., Zhang, L., Wu, X., Qin, W., &Skibniewski, M. J. (2019). Modeling face reliability in tunneling: A copula approach. *Computers and Geotechnics*, *109*, 272-286.

Rahaman, O., & Kumar, J. (2020). Stability analysis of twin horse-shoe shaped tunnels in rock mass. *Tunnelling and Underground Space Technology*, *98*, 103354.

Saikia, P., Baruah, R. D., Singh, S. K., & Chaudhuri, P. K. (2020). Artificial Neural Networks in the domain of reservoir characterization: A review from shallow to deep models. *Computers & Geosciences*, *135*, 104357.

Sloan, S. W. (1988). Lower bound limit analysis using finite elements and linear programming. *International journal for numerical and analytical methods in geomechanics*, *12*(1), 61-77.

Sloan, S. W., & Assadi, A. (1991). Undrained stability of a square tunnel in a soil whose strength increases linearly with depth. *Computers and Geotechnics*, *12*(4), 321-346.

Spanos, P. D., & Ghanem, R. (1989). Stochastic finite element expansion for random media. *Journal of engineering mechanics*, *115*(5), 1035-1053.

Sudret, B., & Der Kiureghian, A. (2000). *Stochastic finite element methods and reliability: a state-of-the-art report* (pp. 18-34). Berkeley: Department of Civil and Environmental Engineering, University of California.

Vanmarcke, E., & Grigoriu, M. (1983). Stochastic finite element analysis of simple beams. *Journal of engineering mechanics*, *109*(5), 1203-1214.

Vořechovský, M. (2008). Simulation of simply cross correlated random fields by series expansion methods. *Structural safety*, *30*(4), 337-363.

Wang, Z. Z., & Goh, S. H. (2021). Novel approach to efficient slope reliability analysis in spatially variable soils. *Engineering Geology*, *281*, 105989.

Yamamoto, K., Lyamin, A. V., Wilson, D. W., Sloan, S. W., & Abbo, A. J. (2011). Stability of a circular tunnel in cohesive-frictional soil subjected to surcharge loading. *Computers and Geotechnics*, *38*(4), 504-514.

Zhang, J., Phoon, K. K., Zhang, D., Huang, H., & Tang, C. (2021). Deep learning-based evaluation of factor of safety with confidence interval for tunnel deformation in spatially variable soil. *Journal of Rock Mechanics and Geotechnical Engineering*, *13*(6), 1358-1367.

Zhang, W., Li, H., Li, Y., Liu, H., Chen, Y., & Ding, X. (2021). Application of deep learning algorithms in geotechnical engineering: a short critical review. *Artificial Intelligence Review*, *54*(8), 5633-5673.

Zhang, Y., Li, M., Han, S., Ren, Q., & Shi, J. (2019). Intelligent identification for rock-mineral microscopic images using ensemble machine learning algorithms. *Sensors*, *19*(18), 3914.